CSIRO Publishing

Publications of the Astronomical Society of Australia

VOLUME 19, 2002

© ASTRONOMICAL SOCIETY OF AUSTRALIA 2002

An international journal of astronomy and astrophysics

For editorial enquiries and manuscripts, please contact:
The Editor, PASA,
ATNF, CSIRO,
PO Box 76,
Epping, NSW 1710, Australia
Telephone: +61 2 9372 4590
Fax: +61 2 9372 4310
Email: Michelle.Storey@atnf.csiro.au

For general enquiries and subscriptions, please contact:
CSIRO Publishing
PO Box 1139 (150 Oxford St)
Collingwood, Vic. 3066, Australia
Telephone: +61 3 9662 7666
Fax: +61 3 9662 7555
Email: publishing.pasa@csiro.au

Published by CSIRO Publishing
for the Astronomical Society of Australia

www.publish.csiro.au/journals/pasa

Publ. Astron. Soc. Aust., 2002, 19, 499–504

Molecular Masers in Variable Stars

Georgij M. Rudnitskij

Sternberg Astronomical Institute*
13 Universitetskij prospekt, Moscow, 119899 Russia
gmr@sai.msu.ru

Received 2002 May 8, accepted 2002 September 17

Abstract: When a star with a mass of one to a few solar masses enters the red giant stage of its evolution, the radius of its atmosphere reaches several astronomical units. Pulsational instability is typical for this stage. Most stars become Mira-type or semiregular variables with light cycles of a few hundred days. Red giants lose mass at a rate $\dot{M} = 10^{-7}$–$10^{-5} M_\odot$ yr^{-1}. Extensive gas–dust circumstellar envelopes form. These envelopes contain various molecular species. Some of these molecules (OH, H_2O, SiO, HCN) manifest themselves in maser radio emission. Data on the H_2O maser variability and its connection with the stellar brightness variations are discussed. In the H_2O line circumstellar masers can be divided into 'stable' (showing persistent emission — R Aql, U Her, S CrB, X Hya) and 'transient' (appearing in the H_2O line once per 10–15 stellar light cycles — R Leo, R Cas, U Aur). Physical mechanisms of the maser variability are discussed. The most probable process explaining the observed visual–H_2O correlation is the influence of shock waves on the masing region. Usually it is assumed that shocks in Mira atmospheres are driven by stellar pulsations. Here an alternative explanation is proposed. If a star during its main sequence life possessed a planetary system, similar to the solar system, the planets will be embedded in a rather dense and hot medium. Effects of a planet revolving around a red giant at a short distance (inside its circumstellar envelope) are discussed. A shock produced by the supersonic motion of a planet can account for the correlated variability of the Hα line emission and H_2O maser. If the planetary orbit is highly eccentric, then the connected Hα–H_2O flare episodes may be explained by the periastron passage of the planet. New tasks for the upgraded ATCA are discussed.

Keywords: stars: late-type — masers — shock waves — extrasolar planets

1 Circumstellar Molecular Masers

At the end of its evolution, a solar-type star enters the phase of a red giant. Its radius grows from $\sim 1 R_\odot$ to a few $10^2 R_\odot$ (Haniff, Scholz, & Tuthill 1995). The star begins to lose matter, and an extensive gas–dust circumstellar envelope forms (Knapp et al. 1982). The red giant stage is very short as compared to the main sequence stage; it takes no more than a few hundred thousand years. The ultimate end is a complete loss of the convective shell, and formation of a naked white dwarf core surrounded by a planetary nebula (Habing 1996).

The masses of the red giants considered are from one to several solar masses, and their luminosities reach a few $10^3 L_\odot$ (Clayton & Feast 1969). Many red giants are variable; their visual brightness changes on timescales of hundreds of days. These stars are referred to as long-period variables (LPVs). The LPV subtypes are (Kholopov et al. 1985–1987):

- periodic Mira Ceti-type stars, or Miras (M), with visual brightness amplitudes $\Delta m > 2.5$ magnitudes, with periods typically between 150 and 600 days;
- semiregular stars (SR); their amplitudes are <2.5 magnitudes, variations are less regular than in Miras and usually have shorter timescales, 50 to 150 days.

The LPV optical spectra are classified as types M, S, C. The conspicuous spectral features in them are strong molecular bands: TiO, VO in M-stars, ZrO in S-stars, CN, C_2 and other carbon-bearing molecules in C-stars. The set of the molecules observed reflects the chemical composition of the stars. In M-stars the O/C atomic number ratio is greater than unity, most carbon atoms are bound in the CO molecules, and the remaining oxygen atoms form oxides. In S-stars O/C ~ 1. In C-stars O/C < 1, all oxygen is in CO, and the rest of the carbon atoms go to carbon-bearing molecules. The M $\rightarrow$ S $\rightarrow$ C sequence probably has an evolutionary meaning (Greene & Wing 1975; Habing 1996). The atomic absorption lines in LPV spectra are rare, the most prominent of them is the resonant line of CaI λ 4227 Å. Sometimes atomic emission lines appear (Balmer series of hydrogen, iron lines, etc.) — probably excited by shock waves (Wood 1979; Gillet, Maurice, & Baade 1983; Fox, Wood, & Dopita 1984). The stars lose matter at a rate $\dot{M} \sim 10^{-7}$–$10^{-5} M_\odot$ yr^{-1} (Knapp et al. 1982). The lost matter forms a circumstellar envelope, containing molecules and dust. Circumstellar dust reradiates stellar light, producing large infrared excesses (Habing 1996).

Circumstellar molecules emit radio lines: thermal rotational lines of CO, SiO, HCN and other molecules (Olofsson et al. 1998), and maser lines (OH, H_2O, SiO, HCN). Circumstellar masers presently known are

- OH $\lambda = 18$ cm (Λ-doubling of the ground rotational state $^2\Pi_{3/2}$, $J = 3/2$: 1612, 1665, 1667 MHz) (Benson et al. 1990);

* http://www.sai.msu.su

© Astronomical Society of Australia 2002
10.1071/AS02018 1323-3580/02/04499$05.00

- H_2O rotational transitions: 6_{16}–5_{23} 22.2 GHz (Benson et al. 1990), 3_{13}–2_{20} 183 GHz (González-Alfonso et al. 1998), 10_{29}–9_{36} 321 GHz (Menten & Melnick 1991), 5_{15}–4_{22} 325 GHz (Yates, Cohen, & Hills 1995);
- SiO $\lambda = 7$, 3.5, 1.7, … mm: rotational transitions $J =$ 1–0, 2–1, 3–2, … in the excited vibrational states $v = 0$, 1, 2, 3, … (Habing 1996);
- HCN $\lambda = 3.4$ mm: rotational transition $J = 1$–0 in the excited vibrational state $v = (0, 2^0, 0)$ (Lucas, Omont, & Guilloteau 1988); $\lambda = 1.1$, 0.85 mm: rotational transitions $J = 3$–2, 4–3 in the excited vibrational state $v = (0, 1^{1c}, 0)$ (Bieging, Shaked, & Gensheimer 2000).

OH and H_2O masers are found in oxygen-rich (M-type) stars; SiO masers in M- and S-type stars; HCN masers in carbon stars. There are a few exceptions: some C-type stars (e.g., EU And, V778 Cyg) host H_2O masers (Little-Marenin, Benson, & Dickinson 1988). Probably, they are M + C binaries or are in a very short transition state from an oxygen-rich to a carbon-rich star.

In this paper, I give special emphasis to the H_2O circumstellar masers, for which we have traced a long-term variability (see Rudnitskij et al. 2000; Lekht et al. 2001 and references therein). Furthermore, H_2O masers are of interest because they trace precisely the region of the circumstellar envelope, where condensation of dust and outward acceleration of the gas–dust mixture begin (Habing 1996).

2 Observations

Since 1980, our team has been monitoring a sample of about 20 Miras* in the H_2O maser line at $\lambda = 1.35$ cm; beginning from 1994 we have also been doing optical spectroscopy of these stars (see Esipov et al. 1999 and references therein).

Extensive statistical data on the H_2O maser variability of the stars suggest that there are two groups of circumstellar H_2O masers.

'*Stable*' *masers*, which have been displaying H_2O maser emission (however, with varying intensity) throughout our observational interval, never falling below our detection threshold (∼10 Jy). Examples are R Aql, U Her, RS Vir. For these stars the H_2O maser variations correlate with the visual light curves, following them with a certain delay $\Delta\varphi$ of about 0.3–0.4 P (P is the brightness variation period). For U Ori this delay, analysed on a time interval of ∼12 P, probably itself varies with a 'superperiod' of ∼9 P (Rudnitskij et al. 2000). A cross-correlation analysis between the visual light curve and H_2O maser variations for the Mira RS Vir (Lekht et al. 2001) shows that actually the correlation is maximum for a delay between the visual and H_2O light curves of 4–5 P. These stars also frequently show Balmer emission lines in their spectra, in nearly every light cycle.

'Transient' masers, which sometimes disappeared from our view, falling below our detection threshold of 10 Jy for certain intervals. Some of them (R Leo, R Cas, U Aur) remained 'H_2O-silent' for more than 15 years, but then episodically reappeared. The Hα emission was seldom observed in these stars, usually in the form of short episodes, lasting a couple of weeks, near selected light minima (Esipov et al. 1999).

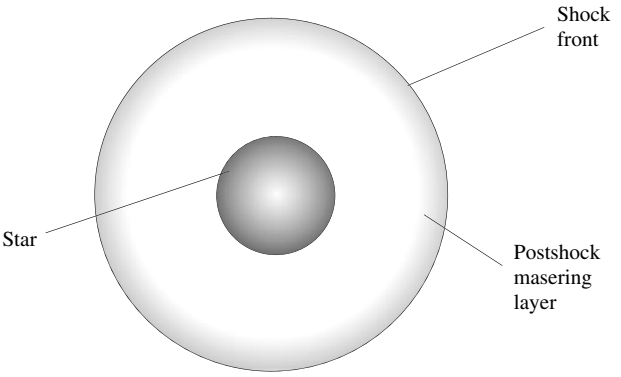


Figure 1 Model of H_2O maser pumping by a spherical shock (Rudnitskij & Chuprikov 1990).

In addition to this, the H_2O masers from both groups display from time to time strong flares, when their H_2O line flux increases a thousandfold. An example is the Mira U Ori. According to our data of March and June 1980, this star was 'silent' in H_2O with the peak flux density below 10–12 Jy. However, between June and October 1980 the U Ori maser brightened to more than 1000 Jy (Berulis et al. 1983; Rudnitskij et al. 2000). Similar events took place in the H_2O maser associated with the Mira-like semiregular variable W Hya in 1981 (Berulis et al. 1983) and in 2001.

The correlation between the visual light curve and the H_2O maser variations can be explained by the model of shock impact on the masing region (Rudnitskij & Chuprikov 1990, Figure 1; see also text below). Shock waves, departing from the stellar surface under the action of pulsations, reach some time after the layers of the circumstellar envelope containing the H_2O molecules. At this, collisional maser pumping is enhanced, and the maser line flux increases. The case of RS Vir suggests that this delay may be as long as a few stellar periods (Lekht et al. 2001), corresponding to a shock velocity of $\sim 10\,\mathrm{km\,s^{-1}}$.

In the star R Leo we have observed in May 1996 a short Hα line flare, followed a year and a half later by a flare in the H_2O radio line (Esipov et al. 1999, Figure 2). On a smaller scale, the same sequence was observed in R Cas and U Aur. All these stars were strong H_2O emitters in the early 1980s, but then faded below our detection limit (∼10 Jy) and remained unobservable to us until recently. The brief reappearance of R Leo in the H_2O line 18 months after the Hα flare was the first episode of this kind we have observed. Unfortunately, there are gaps in our Hα data, and we cannot assert definitely that no similar Hα events, before or after May 1996, have been missed. However, for this particular star, strong Hα emission may be indeed an infrequent phenomenon: Castelaz & Luttermoser (1997)

*http://comet.sai.msu.ru/gmr/miras.html

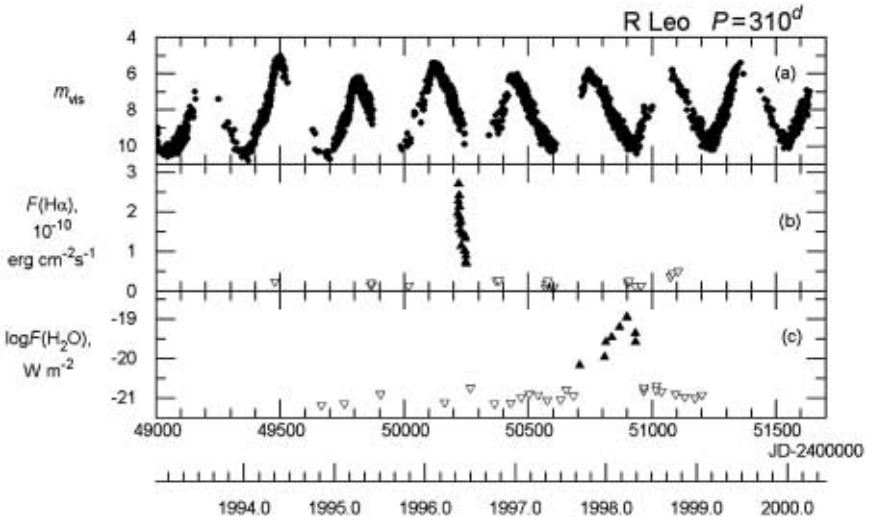


Figure 2 Observations of R Leo: (a) visual light curve (AFOEV data); (b) flux in the Hα emission line; (c) H_2O line flux (Esipov et al. 1999). Open triangles: upper limits.

monitored R Leo spectroscopically at various phases of its light curve and saw a weak Hα emission only once, near light maximum. At the same time, many other stars from their sample and from ours (Esipov et al. 1999) often display rather strong Hα emission, e.g., T CrB, R Tri, T Her, U Her. This gives us reason to believe that we have really observed a rare isolated event in R Leo. Therefore, we have assumed a shock as a common cause of these two flares (Hα and H_2O flares).

If such an event is indeed rare and takes place once per 10–15 stellar light cycles, there can be various explanations. Rudnitskij & Chuprikov (1990) explained this fact by building and disruption of a quasi-stationary layer of gas and dust (QSL), hosting the masing H_2O molecules. QSL is observed in atomic and molecular absorption lines in some Miras, including R Leo, as a component at the stellar radial velocity. QSL is located at a distance of about ten stellar radii from the centre of the star; it may represent a temporary stop of the material leaving the star. In the stars studied QSL can sometimes appear and disappear (Hinkle & Barnes 1979; Hinkle, Scharlach, & Hall 1984). The conditions in QSL ($T \sim 800$ K, $n \sim 10^9$ cm^{-3}) are favourable for H_2O maser action. The H_2O maser pumping is especially enhanced if a shock wave (with a velocity of 6–10 km s^{-1}, a stronger shock would simply dissociate molecules) crosses QSL. Behind the shock the gas is heated almost instantly, whereas some time is required to transfer heat to dust particles. Thus, there is a nonequilibrium post-shock layer with hot gas (source of energy for H_2O maser pumping) and cooler dust (maser energy sink)—see Rudnitskij & Chuprikov (1990) for details. A strong shock produces Balmer emission near the photosphere and, reaching QSL some time later, amplifies the H_2O maser intensity. The passage of attenuated shocks in every light cycle of the star can explain the correlation of the H_2O maser variations with the visual light curve of the star, when the H_2O maser flux follows the optical brightness variations with some delay, see above. QSL can originate in a stronger mass-loss episode once per several stellar cycles. Another cause may be that pulsation-driven shocks, consecutively departing from the stellar surface, can overtake their predecessors and merge with them, thus producing, again once per several cycles, a stronger than average shock (Wood 1979), also resulting in a maser flare. If QSL vanishes for some time, the maser zone may disappear, too, and this accounts for the temporary 'silence' of the maser (as in U Ori).

The main problem may be that shocks in Miras are not so strong as has been believed. Based on the Hα emission line profiles in o Cet, Gillet et al. (1983) inferred shock velocities v_s near the photosphere of up to 90 km s^{-1}. However, other optical spectroscopy data (Fox et al. 1984) and the weakness or lack of microwave continuum, which should accompany the Hα emission (Reid & Menten 1997; Chapman & Rudnitskij 2002), suggest photospheric v_s values no higher than $\sim$20–25 km s^{-1}. This is difficult to reconcile with the intense Balmer emission.

As a basis of a discussion, I propose another explanation for the lack of radio continuum and for the rare Hα–H_2O episodes in the 'transient' H_2O source, namely, impact of a shock provoked by a low-mass companion (a planet?) to the Mira star. This possibility is considered in the next section.

3 Effects of a Relic Planetary System around a Red Giant

If a star possessed a planetary system during its main-sequence life, at the red giant stage the closer planets, revolving at $R \sim 1-3$ AU, will be embedded within the star's atmosphere. The more massive ones will probably survive the red giant phase (Struck-Marcell 1988; Rybicki & Denis 2001).

Evolution of a red giant having a compact stellar companion (a brown/black dwarf with a mass of $\geq 0.02\,M_\odot$ or possibly a neutron star) was analysed in a series of

papers on the 'double-core evolution' (Soker 1999, and references therein). The fate of a lower-mass companion (0.001–0.01 $M_\odot$—a planet), embedded in the atmosphere of a star that has become a red giant, was also considered in a number of works. In particular, Soker (1999) proposed to search for Uranus–Neptune-like planets in planetary nebulae, formed in the course of the post-AGB evolution.

Systematic observations of the last decade have led to discoveries of several tens of planets orbiting solar-type stars in the solar vicinity. Most of them have been detected by the Doppler technique, involving precise measurements of stellar radial velocities on a time interval of several years, aiming to find small velocity shifts caused by the orbital motion of a low-mass companion. Depending on the planet's mass and semimajor axis, amplitudes of such velocity variations are from several $\mathrm{m\,s^{-1}}$ to several scores of $\mathrm{m\,s^{-1}}$. A complete list of these detections* is maintained by Jean Schneider† at the Paris–Meudon Observatory.

Of course the Doppler technique, used on a limited time interval, selects in the first instance more massive planets in orbits closer to the central stars. The planets detected so far can be divided into two groups: (1) 'hot Jupiters', planets of one to a few Jupiter masses, revolving in circular orbits very close to their stars, at 0.05–0.5 AU; (2) planets in eccentric orbits (with e up to 0.6) with revolution periods up to a few hundred days. Certainly, further observations will find lower-mass and longer-period planets, perhaps planetary systems similar to the Solar System.

A planet orbiting around a $1M_\odot$ star at a distance of 1 AU would move at velocity $V_p \sim 30\,\mathrm{km\,s^{-1}}$. If the star is a red giant, then the planet is embedded in the star's atmosphere, having a temperature $T \sim 2000$ K and particle number density of $\sim 10^{12}$–$10^{13}\,\mathrm{cm^{-3}}$. The velocity of sound a_s there would be about $3.4\,\mathrm{km\,s^{-1}}$. Thus, the planet's motion is supersonic, the Mach number $M = V_p/a_s$ being about 9. This motion is similar to the motion of a large meteoritic body in the Earth's atmosphere (Tsikulin 1969). A strong conical shock wave, ionising the gas and heating it to 10,000–15,000 K, is formed.

We consider a simple model, in which a perturbing body with diameter d is moving along a rectilinear trajectory at velocity $V_p > a_s$ through a medium with mass density ρ_0. Quantity E is the energy released at a unit path of the body's motion; E is numerically equal to the drag force exerted on the body by the medium:

$$F = \frac{\pi d^2}{4}\rho_0 V_p^2. \tag{1}$$

Owing to the drag, the planet is gradually spiralling into the red giant's atmosphere. The rate of decrease of its semimajor axis a is (see, e.g., Taam, Bodenheimer, & Ostriker 1978):

$$\frac{\dot a}{a} = -\frac{F V_p a}{G M_* M_p}. \tag{2}$$

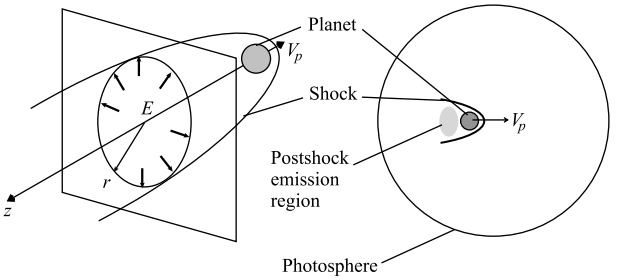


Figure 3 Left: Propagation of a shock wave within a slab perpendicular to the body's velocity vector; E is the energy released in this layer. Right: Motion of a planet across the disc of a red giant at supersonic velocity V_p.

Using (1) and substituting $a = 1$ AU, $M_* = 1M_\odot$, $V_p = 30\,\mathrm{km\,s^{-1}}$, and Jupiter's parameters $M_p = 1M_\mathrm{J} = 1.9 \times 10^{30}$ g, $d = d_\mathrm{J} = 1.4 \times 10^{10}$ cm, we have $\dot a/a \sim -8 \times 10^{-8}\,\mathrm{yr^{-1}}$. Thus, during the red giant stage, which lasts not longer than 10^6 years, the semimajor axis of the planet's orbit decreases by $\leq 8\%$. For a larger planet ($13M_\mathrm{J}$, $2.35d_\mathrm{J}$), braking is still smaller, $\leq 3.2\%$.

The motion of the planet through the stellar atmosphere is similar to the case of propagation of a shock wave from a detonating cylindrical charge (Tsikulin 1969). That is, in any plane perpendicular to the trajectory of the body, the propagating shock can be considered as a cylindrical one (see Figure 3). The shock front radius in this plane is

$$r_f = \left(\frac{E}{\rho_0}\right)^{1/4} t^{1/2} \tag{3}$$

with $t = z/V_p$. The front equation in (r, z) coordinates (Figure 3, left) is

$$\frac{r_f}{d} = \left(\frac{\pi}{4}\right)^{1/4}\left(\frac{z}{d}\right)^{1/2}. \tag{4}$$

Shock velocity D in the direction perpendicular to the trajectory is decreasing with time as

$$D = \frac{1}{2}\left(\frac{E}{\rho_0}\right)^{1/4} t^{-1/2}. \tag{5}$$

For a planet with $d = 2.35d_\mathrm{J}$, velocity D will fall to the velocity of sound a_s at a distance $z_\mathrm{max} = d(\pi/4)^{1/2}(M^2/4) \sim 5.6 \times 10^{11}$ cm behind the body. There will be no emission at greater z. The corresponding maximum front radius $r_{f\,\mathrm{max}} = 1.3 \times 10^{11}$ cm. The maximum projected area of the shocked 'cone' (for a side view, as in Figure 3, right) is

$$S_\mathrm{sh} = \frac{1}{3}(4\pi)^{1/4} d^{1/2} z_\mathrm{max}^{3/2} \sim 4.8 \times 10^{22}\ \mathrm{cm^2} \sim 1.6 \times 10^{-5} S_*, \tag{6}$$

where $S_* = \pi R_*^2 \sim 3 \times 10^{27}\,\mathrm{cm^2}$ is the stellar disc area for $R_* \sim 3 \times 10^{13}$ cm. Observations and model calculations

*http://www.obspm.fr/encycl/catalog.html
†http://www.obspm.fr/schneider/

of the Balmer emission lines in Miras (e.g., Fox & Wood 1985) show that, for the above-mentioned parameters, the shock front yields up to 10^{20} Hα photons cm^{-2} s^{-1}; with source area $S_{\rm sh}$, this can account for the total Balmer line fluxes observed from a star at a distance of about 300 pc, a few $\times 10^{-12}$ erg cm^{-2} s^{-1} (Fox et al. 1984). The side-view observations of the cone shock also naturally explain doubling and large linewidth ($\sim$60 km s^{-1}) of the Balmer lines observed in Miras (e.g., Gillet et al. 1983; Udry et al. 1998). The lack of radio continuum is explained by the small angular size of the planetary source, which is thought hot enough to produce the observed Balmer emission.

Another effect of the planetary shock is enhanced H_2O maser pumping by the mechanism proposed by Rudnitskij & Chuprikov (1990); the delay may be similar to the case of a spherical shock.

As mentioned above, some stars (R Leo, R Cas and U Aur) displayed isolated bursts of Hα emission, followed (about a year and a half later) by a flare of the H_2O maser radio emission. This may be due to a periastron shock wave episode of a planet in a highly eccentric orbit with a period $P \sim 15$ years. Some other stars (e.g., U Ori, Rudnitskij et al. 2000) have already shown some hints of H_2O maser 'superperiodicity' of 12–15 years, which could be associated with planetary revolution periods.

One of the main objections to the model proposed is that the drag of the surrounding medium tends to circularise the planet's orbit. However, Soker (2000) has shown that in the case of a mass-losing central star the passage of the periastron by a planet enhances the mass-loss rate, and this effect can support, and even increase, the orbit eccentricity.

4 What Could Be Done on the Upgraded ATCA?

To test the models of the circumstellar H_2O maser emission proposed above, of interest would be repeated mapping of the masers. This would allow us to trace the propagation of a shock across the maser layer, igniting sequentially maser spots more and more distant from the stellar surface. Then it can be found whether the shock is spherical, as in the model of Rudnitskij & Chuprikov (1990), or connected with a local source (a planet) moving across the stellar disc, and the shocked region trailing after it. A task for the H_2O masers in C-stars (see Section 1) could be precise measurement of the maser position with respect to the optical carbon-rich star, to understand whether the H_2O maser coincides with the star or is somewhat shifted and belongs to an optically obscured oxygen-rich companion. Thus it can be elucidated whether these objects are indeed binaries, consisting of carbon- and oxygen-rich stars, or stars in the transition phase from the oxygen-rich to carbon-rich state, when the photosphere already displays an optical spectrum typical of C-stars and the circumstellar envelope still contains more oxygen than carbon.

Unfortunately, such observations may be feasible only for the nearest stars (e.g., W Hya, $d \sim 90$ pc): the angular diameter of the circumstellar H_2O maser region ($r \sim 10^{14}$ cm) at a distance of 100 pc is 70 milliarcseconds (mas), which is below the ATCA resolution at $\lambda = 1.35$ cm ($\sim 0.5''$).

The situation is better for the shorter-wave SiO and HCN masers; here, mapping at various epochs could detect variations in the brightness and relative positions of individual SiO maser spots, caused by pulsation- (or planet-?) driven shocks, and distinguish the cases of a spherical shock, due to the oscillation of a star as a whole, and a 'one-sided' shock (Figure 3), appearing near the limb and travelling across the stellar disc, with SiO maser spots flaring behind.

Meanwhile, the method described by Plambeck, Wright, & Carlstrom (1990) can be used. Plambeck et al. (1990) observed the 86 GHz SiO maser in Ori IRc2 on the Hat Creek millimetre-wave array with a maximum baseline of 177 m. Measuring cross-correlation phases throughout the SiO spectrum, they obtained relative positions of bright Doppler features to an accuracy of 15 mas. If applied to ATCA, this method may yield relative positions of the H_2O maser spots to a fraction of the ATCA beamwidth, which is to some degree a solution of the stated problem.

Continuum observations of red giants at 1.35 cm and 3 mm can be proposed, similar to those performed on the ATCA at $\lambda = 6$ and 3 cm by Chapman & Rudnitskij (2002). For a thermal spectrum, $F_\nu \propto \nu^2$, and shorter-wave observations are more promising for detection. In the millimetre continuum, flux densities of about a millijansky from red giants may be expected, due to photospheric emission. Episodes connected with shocks can also happen; in this case parallel monitoring in optical spectroscopy is useful for shock diagnostics.

Acknowledgments

I gratefully acknowledge the travel support from the International Astronomical Union and the MNRFIC program. I am also grateful to anonymous referees for helpful comments.

References

Benson, P. J., Little-Marenin, I. R., Woods, T. C., Attridge, J. M., Blais, K. A., Rudolph, D. B., Rubiera, M. E., & Keefe, H. L. 1990, ApJS, 74, 911
Berulis, I. I., Lekht, E. E., Pashchenko, M. I., & Rudnitskij, G. M. 1983, SvA, 27, 179
Bieging, J. J., Shaked, S., & Gensheimer, P. D. 2000, ApJ, 543, 897
Castelaz, M. W., & Luttermoser, D. G. 1997, AJ, 114, 1584
Chapman, J. M., & Rudnitskij, G. M. 2002, PASA, submitted
Clayton, M. L., & Feast, M. W. 1969, MNRAS, 146, 411
Esipov, V. F., Pashchenko, M. I., Rudnitskij, G. M., & Fomin, S. V. 1999, AstL, 25, 672
Fox, M. W., & Wood, P. R. 1985, ApJ, 297, 455
Fox, M. W., Wood, P. R., & Dopita, M. A. 1984, ApJ, 286, 337
Gillet, D., Maurice, E., & Baade, D. 1983, A&A, 128, 384
González-Alfonso, E., Cernicharo, J., Alcolea, J., & Orlandi, M. A. 1998, A&A, 334, 1016
Greene, A. E., & Wing, R. F. 1975, ApJ, 200, 688
Habing, H. J. 1996, A&AR, 7, 97
Haniff, C. A., Scholz, M., & Tuthill, P. G. 1995, MNRAS, 276, 640

Hinkle, K. H., & Barnes, T. G. 1979, ApJ, 234, 548
Hinkle, K. H., Scharlach, W. W. G., & Hall, D. N. B. 1984, ApJS, 56, 1
Knapp, G. R., Phillips, T. G., Leighton, R. B., Lo, K. Y., Wannier, P. G., Wootten, H. A., & Huggins, P. J. 1982, ApJ, 252, 616
Kholopov, P. N., et al. 1985–1987, General Catalogue of Variable Stars. Vols. I–III (Moscow: Nauka)
Lekht, E. E., Mendoza-Torres, J. E., Rudnitskij, G. M., & Tolmachev, A. M. 2001, A&A, 376, 928
Little-Marenin, I. R., Benson, P. J., & Dickinson, D. F. 1988, ApJ, 330, 828
Lucas, R., Omont, A., & Guilloteau, S. 1988, A&A, 194, 230
Menten, K. M., & Melnick, G. J. 1991, ApJ, 377, 647
Olofsson, H., Lindqvist, M., Nyman, L.-Å., & Winnberg, A. 1998, A&A, 329, 1059
Plambeck, R. L., Wright, M. C. H., & Carlstrom, J. E. 1990, ApJ, 348, L65
Reid, M. J., & Menten, K. M. 1997, ApJ, 476, 327
Rudnitskij, G. M., & Chuprikov, A. A. 1990, SvA, 34, 147
Rudnitskij, G. M., Lekht, E. E., Mendoza-Torres, J. E., Pashchenko, M. I., & Berulis, I. I. 2000, A&AS, 146, 385
Rybicki, K. R., & Denis, C. 2001, Icarus, 151, 130
Soker, N. 1999, MNRAS, 306, 806
Soker, N. 2000, A&A, 357, 557
Struck-Marcell, C. 1988, ApJ, 330, 986
Taam, R. E., Bodenheimer, P., & Ostriker, J. P. 1978, ApJ, 222, 269
Tsikulin, M. A. 1969, Shock Waves Induced in the Atmosphere by Motion of Large Meteoritic Bodies (Moscow: Nauka) (in Russian)
Udry, S., Jorissen, A., Mayor, M., & Van Eck, S. 1998, A&AS, 131, 25
Wood, P. R. 1979, ApJ, 227, 220
Yates, J. A., Cohen, R. J., & Hills, R. E. 1995, MNRAS, 273, 529